Journal of Applied Mechanics and Technical Physics, Vol. 44, No. 5, pp. 626–633, 2003

EVOLUTION OF CONTROLLED DISTURBANCES IN THE SHOCK LAYER ON THE COMPRESSION SURFACE

V. M. Aniskin and S. G. Mironov

UDC 532.526.013+533.6.011.5

Results of an experimental study of density-wave characteristics in the shock layer are presented for the case of a hypersonic nitrogen flow around a model with a two-dimensional compression surface, which is an arc of a circle, and a sharp leading edge. Controlled periodic disturbances developed on the streaky structure are registered by the electron-beam fluorescence technique. The streaky structure of the type of two vortices rotating in the opposite directions is generated in the shock layer by an oblique gas-dynamic whistle.

Key words: *hypersonic flow, streaky structures, shock-layer stability.*

One of the important research directions of the laminar–turbulent transition is the study of evolution of disturbances in a hypersonic boundary layer on compression surfaces. A description of the transition to turbulence under these conditions is a complicated problem, since it is necessary to take into account the effect of the Görtler instability and traveling disturbances of the boundary layer. An even more complicated problem is a description of flow instability at high hypersonic Mach numbers and moderate Reynolds numbers, when the boundary-layer flow on the compression surface is in the form of a viscous shock layer. Flow stability is affected by the close distance between the shock wave and the viscous boundary-layer edge and by significant nonparallelism of the mean flow field. The evolution of disturbances in a hypersonic boundary layer on compression surfaces in the presence of centrifugal and convective instability was considered theoretically in [1, 2]; the problem was solved in the approximation of infinitely high Reynolds numbers. Conditions most similar to the conditions of the viscous shock layer were considered in [3], where the interaction of the Görtler vortices and acoustic instability mode was simulated numerically. The closeness of the shock wave, however, was ignored in [3], and a significant effect of the shock wave on stability was discovered in [4, 5]. There are no experimental investigations of stability of the boundary-layer flow on compression surfaces. One can only note the papers [6, 7], where the development of periodic traveling disturbances on the streaky structure in the shock layer on a flat plate was considered. In the case of surface curvature and positive pressure gradient, however, one should expect substantial changes in the process of disturbance development. It seems also of interest to study the effect of the temperature factor on stability of such flows.

In the present work, we study the characteristics of periodic traveling disturbances of density in a hypersonic shock layer on the compression surface, which is an arc of a circle, in the presence of a developed streaky structure, such as a pair of vortices rotating in the opposite directions, and significant variation of the temperature factor.

1. Model, Experimental Equipment, and Measurement Technique. The model was a two-dimensional compression surface shaped as an arc (with a width of 0.1 m, length of 0.15 m, and maximum thickness of 0.022 m) and made of blackened aluminum. The radius of the compression surface was $R = 0.28$ m, and the arc length was 0.11 m. The nose part of the model was a one-sided wedge with an initial angle equal to 7°; the wedge smoothly transformed into the compression surface at a distance of 0.015 m. The nose bluntness was 0.1 mm. The maximum angle of the radius surface to the flow direction was 20.5°.

Institute of Theoretical and Applied Mechanics, Siberian Division, Russian Academy of Sciences, Novosibirsk 630090. Translated from Prikladnaya Mekhanika i Tekhnicheskaya Fizika, Vol. 44, No. 5, pp. 29–37, September–October, 2003. Original article submitted December 30, 2002.

 0021-8944/03/4405-0626 $25.00

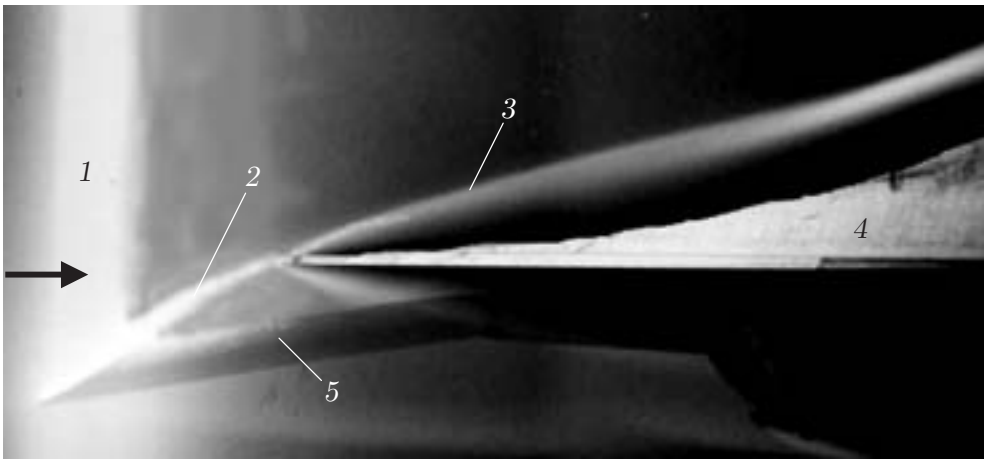

Fig. 1. Electron-beam visualization of the density field in the flow around the model: 1) electron-beam region; 2) shock wave induced by the whistle; 3) shock layer on the model; 4) model; 5) whistle.

Inside the model, there were channels for the cooling liquid. The model temperature was controlled by a built-in copper–Constantan thermocouple. A cylindrical gas-dynamic whistle (with outer and inner diameters equal to 8 and 6 mm, respectively) with a 20° cut-off angle of the front face was attached to the flat part of the model along the longitudinal axis of symmetry. The whistle centerline was established at an angle of 9° to the flow direction to obtain the maximum amplitude of pressure fluctuations. The model is shown on the photograph obtained by electron-beam visualization of the density field (Fig. 1). The structure and operation principle of the gas-dynamic whistle are described in [8]. The resonator of the whistle contained an I-4301 piezoceramic gauge of pressure fluctuations with a limiting frequency of 60 kHz. The signal of this gauge was used to control the frequency and intensity of pressure fluctuations inside the whistle and as a reference signal.

The experiments were performed in a T-327A hypersonic nitrogen wind tunnel of the Institute of Theoretical and Applied Mechanics of the Siberian Division of the Russian Academy of Sciences for a Mach number $M_\infty = 21$, unit Reynolds number $Re_{1\infty} = 6 \cdot 10^5$ m^{-1}, and stagnation temperature of the flow $T_0 = 1150$ K. The basic measurements were performed within the temperature-factor ranges $T_w/T_0 = 0.26$–0.28 and $T_w/T_0 = 0.07$–0.085, since it was possible to obtain stable regimes for the model temperature in these ranges. The lower range of the temperature factor was obtained by using liquid nitrogen as a coolant.

Controlled steady disturbances of the mean flow had the form of two vortices rotating in the opposite directions with imposed periodic disturbances of the varicose type. They were introduced into the shock layer from the model nose with the help of the gas-dynamic whistle by the technique described in [6, 7]. The spectrum of pressure fluctuations inside the whistle contained oscillations at the fundamental frequency and harmonic frequency. Introduction of a developed streaky structure into the shock layer allows one to investigate the development and mutual effect of quasi-steady disturbances of the mean flow and unsteady traveling waves. Under conditions of a high-velocity viscous flow obtained in the present experiment, spontaneous origination of vortex structures was little probable, since the model length was insufficiently large. It was demonstrated in [7] that the artificial traveling disturbances introduced by the whistle propagate over the streaky structure in the form of two-dimensional waves whose spectra in terms of transverse wavenumbers are rather wide because of the finite transverse size of the streaky structure.

The fields of mean density and density fluctuations were measured by the electron beam by the technique adapted to two-dimensional models and described in detail in [9]. The optical system of registration of electron-beam fluorescence of nitrogen is also described there. The flow field was scanned with respect to three coordinates: in the streamwise direction (X coordinate), across the shock layer, normal to the flat base of the model (Y coordinate), and in the transverse direction relative to the X coordinate, coinciding with the electron-beam axis (Z coordinate). Scanning along the X coordinate was performed by moving the model along the flow with respect to the electron beam. Scanning along the Y coordinate was performed by parallel displacement of the beam across the flow with the help of a special magnetic system. Scanning along the Z coordinate was performed by moving the optical system along the electron beam. During wind-tunnel operation, the signals of the optical system and traversing gears were recorded to a multichannel measurement magnetograph, digitized, and processed on a CAMAC-PC system.

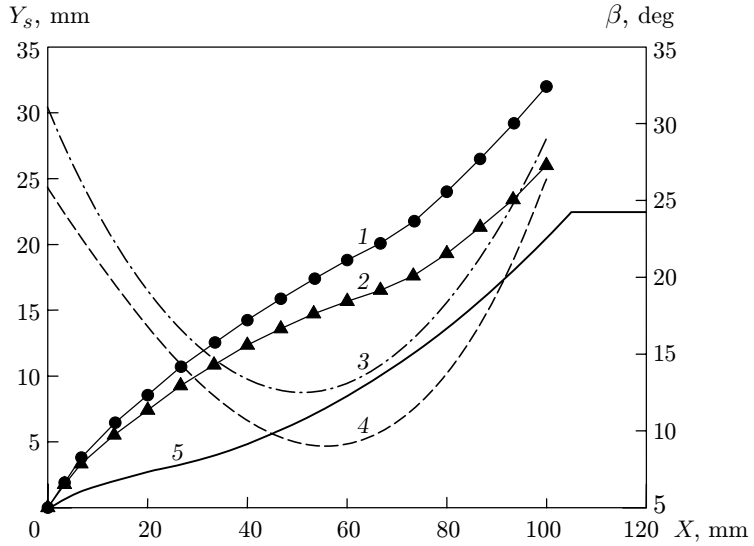

Fig. 2. Position of the shock wave (1 and 2) and angle of shock-wave inclination toward the flow (3 and 4) versus the X coordinate for $T_w/T_0 = 0.26$–0.28 (curves 1 and 3) and 0.07–0.085 (curves 2 and 4); curve 5 shows the coordinates of the model surface.

Processing of raw data reduced to calculation of mutual amplitude and phase spectra of the variable component of nitrogen-fluorescence intensity and the signal of the gauge for pressure fluctuations inside the whistle. Signal fluctuations caused by background disturbances of the wind-tunnel flow were eliminated from the spectra. The mutual amplitude spectra were normalized to the signal of the gauge for pressure fluctuations to eliminate the influence of variation of intensity of pressure fluctuations inside the whistle on the measurement results.

Based on the measured data, we determined the distribution of the mean density in the shock layer and the amplitude and phase of fluctuations of controlled density disturbances at frequencies of pressure fluctuations inside the whistle. The phase was counted from the phase of pressure fluctuations inside the whistle. From the dependences of the relative phase of fluctuations on the X coordinate, we calculated the longitudinal phase velocity for each frequency of disturbances introduced into the shock layer.

2. Measurement Results. Visualization of the limiting streamlines with the help of a vacuum oil/chalk mixture shows that a typical picture is formed on the model surface; it corresponds to origination of a streaky structure and contains a converging line similar to that arising on a flat plate [7]. Measurements of this kind were not performed on the model cooled by nitrogen, but the presence of the same structure was implied.

Figure 2 shows the shock-wave position as a function of the X coordinate in the hypersonic flow around the model. The Y coordinate was counted from the flat part of the model. The data were obtained from the photographs of the flow around the model; one of them is given in Fig. 1. Figure 2 also shows the local angle of inclination of the shock wave toward the free stream β versus the X coordinate, which was calculated from the dependence $Y_s(X)$. The data in Figs. 2–6 were obtained for the plane passing through the longitudinal axis of symmetry of the model ($Z = 0$). Model cooling decreases the shock-layer thickness and local angles of shock-wave inclination toward the free-stream direction. The mean (over the measurement range) Mach number behind the shock wave is estimated by the Hugoniot adiabat relations in a perfect gas as $\mathrm{M}_e \simeq 7.5$ for the "warm" model and $\mathrm{M}_e \simeq 9$ for the model cooled by liquid nitrogen; the values of the Görtler number are $\mathrm{G} = 9.0$ and 9.5, respectively.

The possibility of flow separation from the compression surface was evaluated by the data of [10], where an empirical dependence is given for the minimum angle of laminar separation β_i versus the rarefaction parameter $V_\infty = \mathrm{M}_\infty (C^*/\mathrm{Re}_{x\infty})^{1/2}$ for a corner configuration of the compression surface ($\mathrm{Re}_{x\infty}$ is the local Reynolds number based on the free-stream parameters and $C^* \simeq 0.8$ is the Chapman–Rubezin constant). The dependence $\beta_i \simeq 80(V_\infty)^{1/2}$ yields $\beta_i \simeq 21.5°$, which indicates a low probability of separation even at the end of the arc of the model surface.

Flow rarefaction decreases the density difference on the shock wave and, hence, the temperature difference. The influence of rarefaction is manifested for $V_\infty > 0.1$ [11]. In addition, the effect of gas slipping on the surface

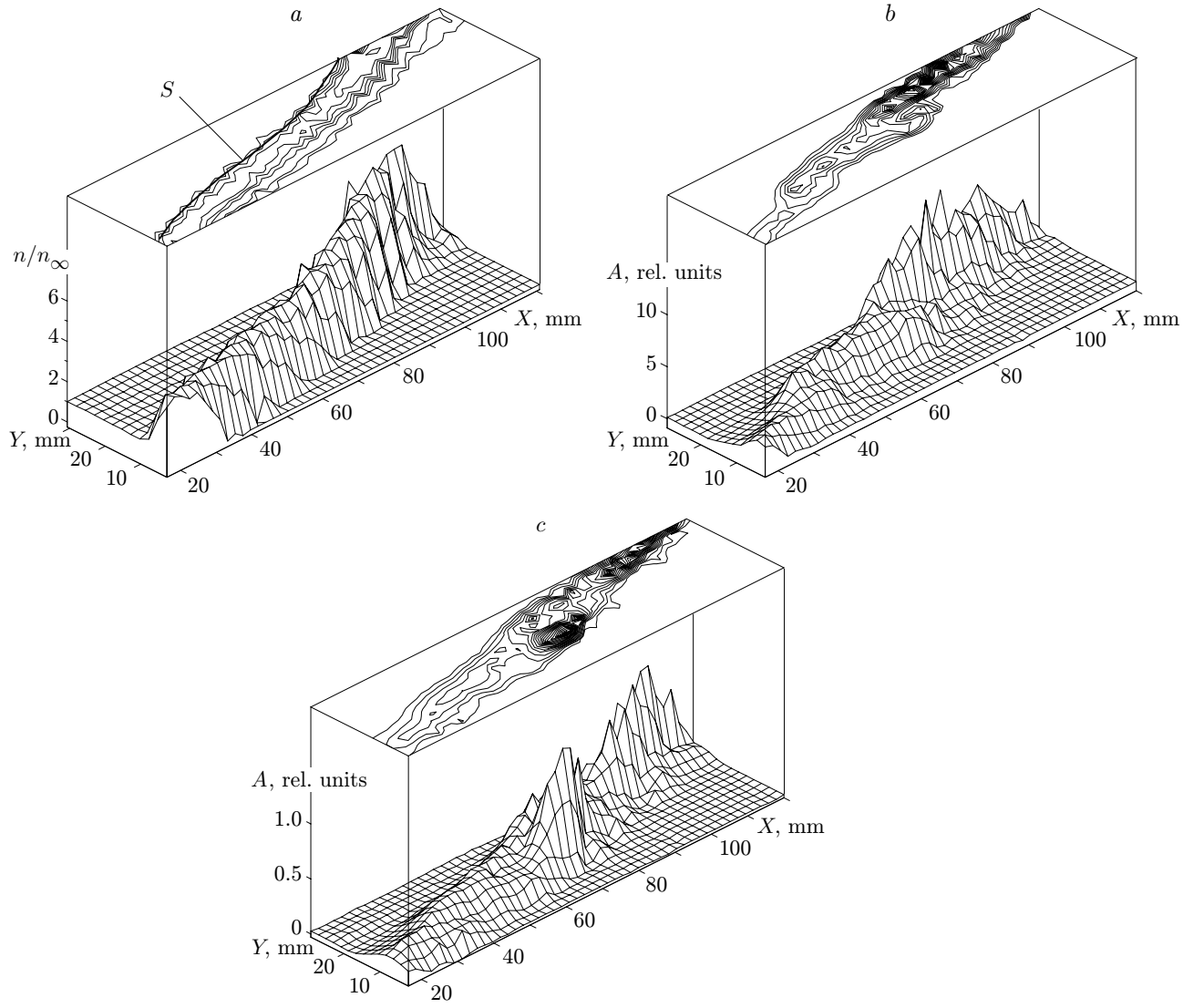

Fig. 3. Distributions of the mean density in the shock layer (a) and density fluctuations at the fundamental frequency (b) and harmonic frequency (c) for $T_w/T_0 = 0.26$–0.28 (S is the shock-wave position).

is observed in this region. Under conditions of the present work, the value of V_∞ becomes lower than 0.1 at a distance from the model tip approximately equal to 0.05 m. Therefore, the static temperature distribution along the surface arc is nonuniform, and the values of temperature differ from those on the shock adiabat. Therefore, the mean density field was "reconstructed" in two stages. First, the density was calculated from the measured results of fluorescence intensity and calibration dependences for temperatures calculated by the shock-wave inclination angle and relations on the Hugoniot adiabat. Then, the static temperature behind the shock wave was calculated again from the resultant values of density and Hugoniot adiabat relations. After that, the density for these values of static temperature was determined.

Figure 3a shows a typical distribution of the relative mean density (concentration of nitrogen molecules) n/n_∞ measured for $T_w/T_0 = 0.26$–0.28 and also the shock-wave position obtained by flow visualization. The shock-wave line is located in the middle of the external region of the mean-density distribution. Smearing of the density-difference front is caused by the finite width of the electron beam.

The measurement of density distributions along the Z coordinate in the region of shock-wave location show that the presence of the streaky structure leads to a decrease in the mean density at the centerline of the streaky structure on the sector turned toward the model and to an increase in the mean density on the sector turned away from the model. This corresponds to bending of the shock-wave surface away from the model under the action of

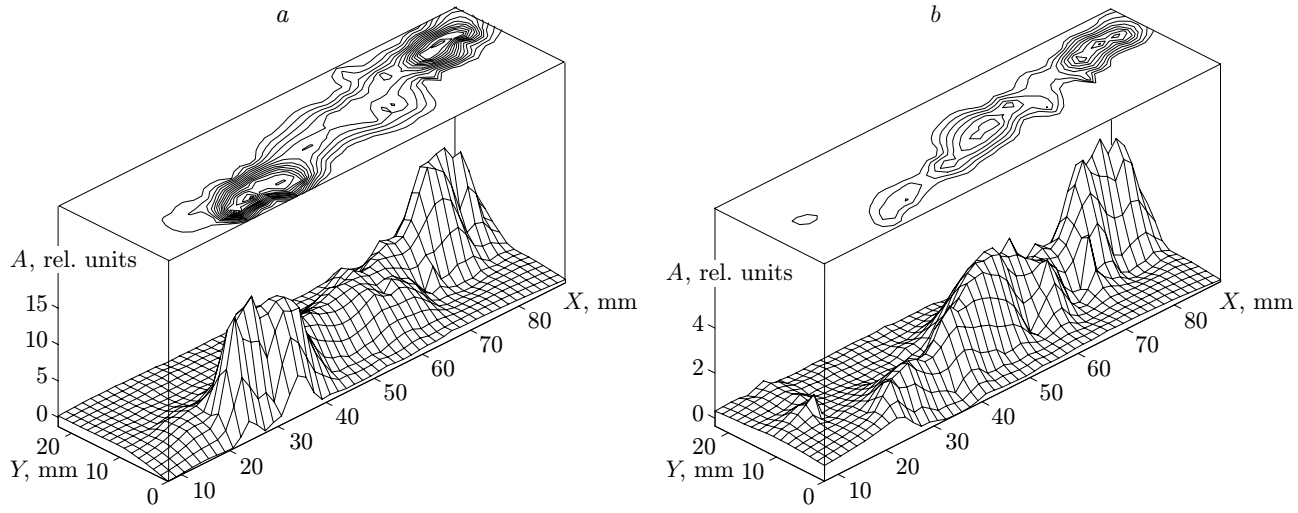

Fig. 4. Distribution of density fluctuations at the fundamental frequency (a) and harmonic frequency (b) for $T_w/T_0 = 0.07$–0.085.

ascending gas flows generated by the pair of vortices rotating in the opposite directions. The width of the mean flow field deformation region varies little along the model and reaches approximately 20 mm. The same value was obtained in [6, 7].

Figure 3 shows the distributions of the amplitude of density fluctuations A over the shock layer at the fundamental frequency $f = 8.6$ kHz (b) and harmonic frequency $f = 17.2$ kHz (c). These frequencies correspond to the values of the dimensionless frequency parameter $F = 2\pi f/(\mathrm{Re}_{1\infty} U_\infty) = 0.6 \cdot 10^{-4}$ and $1.2 \cdot 10^{-4}$, respectively (the value of $\mathrm{Re}_{1\infty}$ was determined by the free-stream parameters). The maximums of fluctuations are located close to the shock wave; the amplitude of fluctuations at the fundamental frequency increases monotonically along the generatrix of the compression surface and decreases at the horizontal sector at the end of the model ($X > 0.105$ m). The curve $A(x)$ at the harmonic frequency has two increasing sectors: on the arc and on the horizontal part of the model.

Figure 4a and b shows the distributions of density fluctuations for the "cold" model for $F = 0.49 \cdot 10^{-4}$ and $0.98 \cdot 10^{-4}$, respectively. In contrast to the "warm" model, the dependence is significantly nonmonotonic, and the change in amplitude occurs at a smaller sector over the X coordinate; the distributions are characterized by two clear maximums.

Figure 5 shows the growth rate of disturbances α_i on the surface versus the X coordinate. The growth rate was determined in a standard manner for points located in a vicinity of the maximum of the distribution of fluctuations in Fig. 3b and c with allowance for the nonuniform distribution of the parameter $\sqrt{\mathrm{Re}_{xe}}$ along the generatrix (Re_{xe} is the local Reynolds number behind the shock wave). The distribution of the local Reynolds number along the generatrix necessary to determine the growth rate was calculated from the experimental values of the local difference in density (the maximum value of density was used for each value of X) and temperature calculated for the corresponding difference in density. It should be noted that the growth rate of disturbances depends substantially on the longitudinal coordinate, and the value of α_i is significantly greater than the growth rate of background disturbances on a flat plate [9], though it does not reach the values obtained in [6, 7] for identical test conditions and frequencies on the streaky structures on a flat plate.

Phase measurements show that traveling disturbances of two types with significantly different values of the streamwise phase velocity C_x propagate in the shock layer. (The quantity C_x is normalized to the mean velocity behind the shock wave U_e.) For each frequency, there are two phase dependences (points 1 and 2 in Fig. 6). The dependences are constructed on the basis of points for which the statistical error of phase determination is smaller than 0.2–0.3 rad. The statistical error of the phase is evaluated by the relation $\Delta\varphi = \sqrt{(1-\gamma^2)/(2\gamma^2 N)}$, where γ^2 is the squared coherence spectrum and $N = 64$ is the number of averagings in amplitude and phase calculations. The points with a low statistical error are located near the maximum of intensity of the distribution of fluctuations (see Figs. 3 and 4), since we have $\gamma^2 \simeq 1$ for intense fluctuations. The phase shift of the dependences is rather close

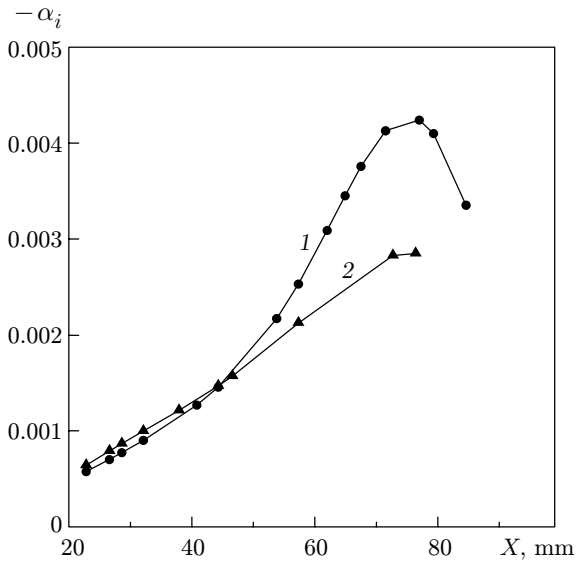

Fig. 5. Growth rate of disturbances versus the X coordinate in the shock layer at the fundamental frequency (1) and harmonic frequency (2) for $T_w/T_0 = 0.26$–0.28.

TABLE 1

T_w/T_0	$F \cdot 10^4$	Number of the phase dependence in Fig. 6	C_x
0.26–0.28	0.6	1*	0.93 ± 0.02
		2	1.60 ± 0.14
	1.2	1*	1.09 ± 0.06
		2*	0.95 ± 0.08
0.07–0.085	0.5	1	0.85 ± 0.045
		2	1.29 ± 0.11
	1.0	1	1.27 ± 0.11
		2	1.27 ± 0.10

Note. For the regime with subsonic disturbances, the number of the phase dependence is marked by an asterisk.

to π. A similar effect was previously obtained in experiments in the wake behind a gas-dynamic whistle [12]. The phase shift in [12], however, was closer to π, which was explained by radial fluctuations of the wake flow and by origination of two regions of fluctuations in the external and internal parts of the mean-density distribution.

The streamwise phase velocities of disturbances for each group of points listed in Table 1 were calculated from the linear approximations of phase dependences (straight lines in Fig. 6). It follows from Table 1 that the shock layer contains both subsonic disturbances, whose phase velocity is within the interval $1 \pm 1/\mathrm{M}_e$, and supersonic disturbances, whose velocity is outside this interval. According to the linear theory of stability of compressible gas flows [13], the boundaries of the interval separate the regions of existence of two-dimensional vortex (subsonic) and acoustic (supersonic) modes. It also follows from Table 1 that both subsonic and supersonic disturbances are formed on the model with higher values of the temperature factor, whereas only supersonic disturbances are observed in the cooled model. An analysis of experimental data in Fig. 6 shows that subsonic disturbances are concentrated in the external region of the distribution of fluctuations and supersonic disturbances are concentrated in the internal region of the shock layer.

The existence of two types of disturbances at one frequency can be attributed to vortex-mode disturbances propagating in the temperature transitional layer with a velocity close to the external flow velocity and generating, in turn, acoustic disturbances. The latter propagate at an angle to the flow direction because of the supersonic velocity of vortex perturbations with respect to lower and slower gas layers.

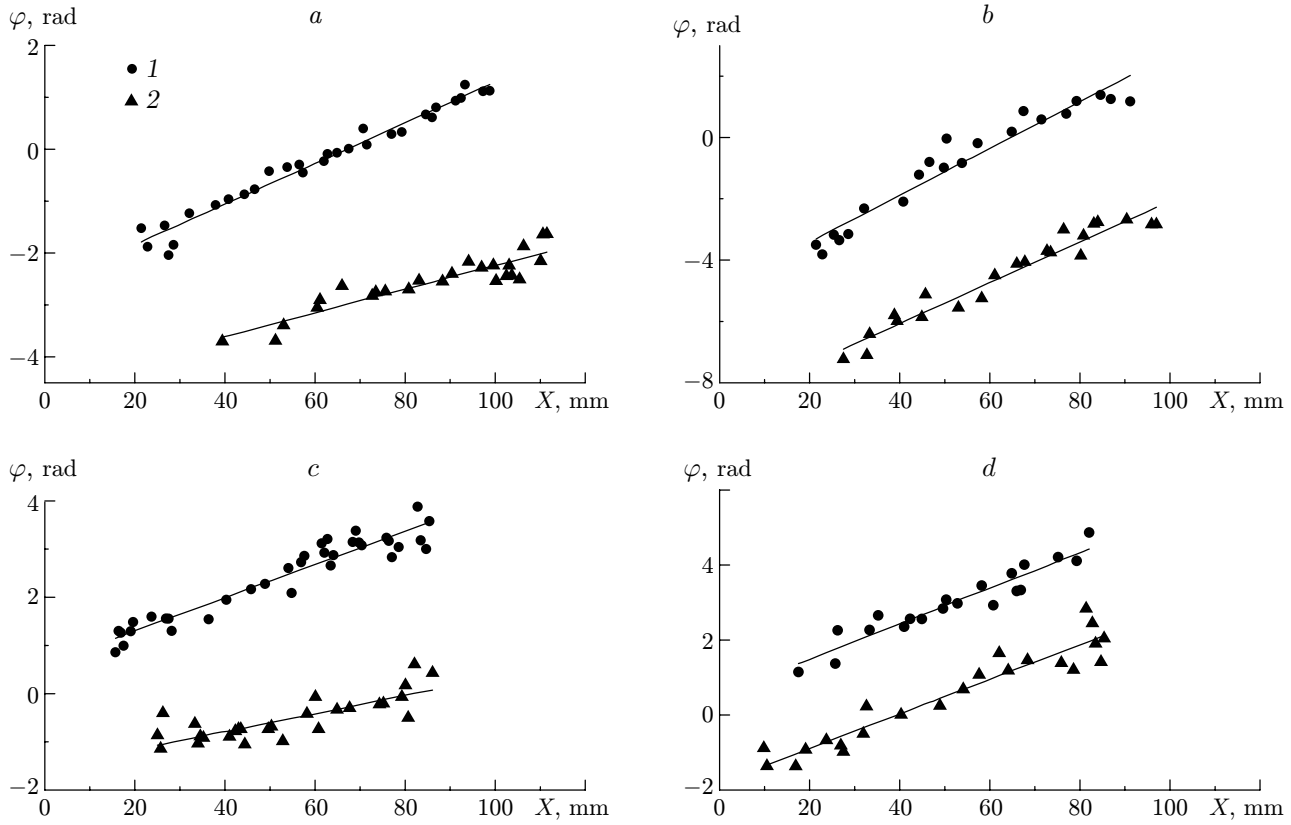

Fig. 6. Relative phase of density fluctuations on the X coordinate for $T_w/T_0 = 0.26$–0.28 (a and b) and 0.07– 0.085 (c and d) and $F = 0.6 \cdot 10^{-4}$ (a), $1.2 \cdot 10^{-4}$ (b), $0.49 \cdot 10^{-4}$ (c), and $0.98 \cdot 10^{-4}$ (d); points 1 and 2 refer to different types of the phase dependence.

Conclusions. It is shown that the thickness of the hypersonic boundary layer and the angle of inclination of the shock wave toward the flow direction decrease with decreasing temperature factor in the flow around a compression surface.

Subsonic and supersonic disturbances of density are found in the shock layer; for low values of the temperature factor, only supersonic (acoustic) disturbances are observed.

For the temperature factor $T_w/T_0 = 0.26$–0.28, a monotonic increase in disturbances both at the fundamental frequency and at the harmonic frequency is observed on a considerable part of the compression arc. For $T_w/T_0 =$ 0.07–0.085, the length of the region of monotonic growth of disturbances is significantly smaller, and two maximums of density fluctuations are observed.

This work was supported by the Russian Foundation for Fundamental Research (Grant Nos. 01-01-00189 and 02-01-00141) and INTAS (Grant No. 2000-0007).

REFERENCES

1. Y. Fu and Ph. Hall, "Nonlinear development and secondary instability of large-amplitude Görtler vortices in hypersonic boundary layer," *Europ. J. Mech. B*, **11**, No. 4, 465–510 (1992).
2. Y. Fu and Ph. Hall, "Effect of Görtler vortices, wall cooling and gas dissociation on the Rayleigh instability in a hypersonic boundary layer," *J. Fluid Mech.*, **247**, 503–525 (1993).
3. C. W. Wang and X. Zhong, "Nonlinear interaction of Görtler and secondary shear modes in hypersonic boundary layers," AIAA Paper No. 2000-0536 (2000).
4. G. V. Petrov, "Stability of a thin viscous layer on a wedge in hypersonic flow of a perfect gas," in: *Laminar–Turbulent Transition*, Proc. of the 2nd IUTAM Symp. on Laminar–Turbulent Transition (Novosibirsk, July 9–13, 1984), Springer-Verlag, Berlin–Heidelberg–New York–Tokyo (1984), pp. 487–493.

5. C. L. Chang, M. R. Malik, and M. Y. Hussaini, "Effects of shock on the stability of hypersonic boundary layers," AIAA Paper No. 90-1448 (1990).
6. S. G. Mironov, "Experimental study of vortex structures in a hypersonic shock layer on a flat plate," *J. Appl. Mech. Tech. Phys.*, **40**, No. 6, 1029–1035 (1999).
7. S. G. Mironov and A. A. Maslov, "Experimental study of secondary instability in a hypersonic shock layer on a flat plate," *J. Fluid Mech.*, **412**, 259–277 (2000).
8. A. A. Maslov and S. G. Mironov, "Experimental investigation of a hypersonic low-density flow around a semi-closed cylindrical cavity," *Izv. Ross. Akad. Nauk, Mekh. Zhidk. Gaza*, No. 6, 155–160 (1996).
9. S. G. Mironov and A. A. Maslov, "An experimental study of density waves in hypersonic shock layer on a flat plate," *Phys. Fluids, A*, **12**, No. 6, 1544–1553 (2000).
10. D. A. Needham and J. L. Stollery, "Boundary layer separation in hypersonic flow," AIAA Paper No. 66-455 (1966).
11. P. J. Harbour and J. H. Lewis, "Preliminary measurements of the hypersonic rarefied flow field on a sharp plate using electron beam probe," in: *Rarefied Gas Dynamics*, Suppl. 2, Acad. Press, New York (1967), pp. 1031–1046.
12. V. M. Aniskin and S. G. Mironov, "Experimental investigation of finite-amplitude waves in a hypersonic wake," *Teplofiz. Aéromekh.*, **8**, No. 2, 345–352 (2001).
13. L. M. Mack, "Boundary layer stability theory," Report No. 900-277, Jet Propulsion Lab., Pasadena, Cal. (1969).